



THE UNIVERSITY *of* EDINBURGH

Edinburgh Research Explorer

VAPB interacts with and modulates the activity of ATF6

Citation for published version:

Gkogkas, C, Middleton, S, Kremer, AM, Wardrope, C, Hannah, M, Gillingwater, TH & Skehel, P 2008, 'VAPB interacts with and modulates the activity of ATF6', *Human Molecular Genetics*, vol. 17, no. 11, pp. 1517-1526. <https://doi.org/10.1093/hmg/ddn040>

Digital Object Identifier (DOI):

[10.1093/hmg/ddn040](https://doi.org/10.1093/hmg/ddn040)

Link:

[Link to publication record in Edinburgh Research Explorer](#)

Document Version:

Peer reviewed version

Published In:

Human Molecular Genetics

Publisher Rights Statement:

Publisher version: <http://hmg.oxfordjournals.org/content/17/11/1517>

© The Author 2008. Published by Oxford University Press. All rights reserved

General rights

Copyright for the publications made accessible via the Edinburgh Research Explorer is retained by the author(s) and / or other copyright owners and it is a condition of accessing these publications that users recognise and abide by the legal requirements associated with these rights.

Take down policy

The University of Edinburgh has made every reasonable effort to ensure that Edinburgh Research Explorer content complies with UK legislation. If you believe that the public display of this file breaches copyright please contact openaccess@ed.ac.uk providing details, and we will remove access to the work immediately and investigate your claim.



VAPB interacts with and modulates the activity of ATF6Christos Gkogkas¹Susan Middleton¹Anna M. Kremer¹Caroline Wardrope¹Matthew Hannah²Thomas H. Gillingwater¹Paul Skehel^{1*}

1. The Centre for Neuroscience Research, The University of Edinburgh, The Hugh Robson Building, George Square, Edinburgh EH8 9XD. UK.
2. Division of Molecular Neuroendocrinology, Medical Research Council, National Institute for Medical Research, The Ridgeway, Mill Hill, London, NW7 1AA, UK.

* To whom correspondence should be addressed.

Tel: 0131 651 1961

Fax: 0131 650 6530

email: paul.skehel@ed.ac.uk

Introduction.

A dominantly inherited familial form of motor neuron disease characterized in a large Brazilian family was recently shown to be associated with a mis-sense mutation in the human *vapB* gene (1). Affected individuals suffer from three different pathological conditions; a late on-set slowly progressing spinal muscular atrophy (SMA), a slowly progressing late on-set atypical amyotrophic lateral sclerosis ALS8, or a typical severe rapidly progressing ALS (2, 3). Although familial forms of disease may represent less than 5% of the total incidences of ALS (4, 5), they exhibit the same phenotypic heterogeneity as the more common sporadic disease (6-8). Information on the mechanistic basis of familial motor neuron diseases may, therefore, be relevant to all forms of motor neuron disease.

The first VAP protein was identified in *Aplysia californica* from its interaction in a yeast two-hybrid screen with VAMP/Synaptobrevin, hence the nomenclature VAMP/Synaptobrevin Associated Protein (9). VAP proteins are highly conserved, with homologous proteins found in all eukaryotes (10-15). There are two mammalian genes *VapA* and *VapB* (16). The proteins contain three prominent structural features; the N-terminal domain of approximately 120 amino acids is highly homologous to the nematode Major Sperm Protein (MSP) (17), the central domain is amphipathic and predicted to form a coiled-coil structure, and the C-terminal 20 amino acids are hydrophobic and act as an intracellular membrane anchor (13, 15, 16).

The MSP domain binds to the “two phenylalanines in an acid tract”, or "FFAT" motif found in several cytoplasmic lipid binding proteins (18-20). The structural basis of this interaction was recently determined for the MSP domain of VAPA (21). Thus,

VAP proteins may act as docking sites for cytoplasmic factors to interact with the ER. VAP proteins may also act to maintain the structure of intracellular membranes such as the ER, by interacting with the cytoskeleton and mediating membrane trafficking (13, 15, 22).

The disease-associated mutation in ALS8 is a C to T substitution within exon 2 of the *vapB* gene replacing a proline residue with a serine in a highly conserved region of the protein. The mutant protein, VAPB^{P56S}, forms aggregates when expressed in cultured cell lines or primary hippocampal neurons (1). The relationship of these aggregates to the pathological mechanism of the disease is not known. It has been suggested that the presence of aggregates containing VAPB^{P56S} may result in disruption of the proteasome, activation of ER stress responses, fragmentation of the Golgi apparatus, and induction of apoptosis (23). Teuling *et al.*, have also demonstrated that expression of VAPB^{P56S} recruits the wild type protein into aggregates and causes disruption of ER structure (24).

In this report we show that both VAPA and VAPB are ubiquitously expressed but at differing levels in different tissues and that they accumulate on overlapping but distinct regions of the ER. Both VAPA and VAPB are shown to be capable of interacting with the ER stress regulated transcription factor ATF6, and over expression of VAPB or VAPB^{P56S} attenuates the activity of an ATF6/XBP1 regulated promoter. This suggests that VAPB can have an inhibitory affect on ATF6 dependent transcription and that the disease associated mutant, VAPB^{P56S}, has an enhanced inhibitory activity towards ATF6-dependent transcription compared to the wild-type protein. An interaction between VAP proteins and ATF6 may represent a previously uncharacterised mechanism of ER homeostatic and stress response regulation.

It is concluded that mis-regulation of ER stress response and homeostatic regulatory systems may contribute to the pathological mechanism of degenerative motor neuron disease associated with the VAPB^{P56S} mutation.

Results.

VAPA and VAPB are expressed ubiquitously but at differing levels in different tissues.

Immunoblot analysis of selected tissues from an adult male rat demonstrated that both VAPA and VAPB proteins are present in all tissues examined, but at different relative levels (Fig1A). This is in agreement with the wide expression profile of mRNA published previously (13, 16, 25). A second protein of slightly larger molecular weight is detected in the testis by VAPA anti-sera. An additional, less abundant, protein of approximately 14kD is detected by both anti-serum. The VAPB-related signal is a doublet, the expression of which is tightly restricted to the forebrain and cerebellum extracts, and not detected in the other tissues tested (Fig1A). The 14kD VAPA-related polypeptide is more widely expressed and detectable in pancreas, liver, forebrain, lung and thymus, kidney and testis; low levels are seen in the cerebellum and no signal is detected in heart or skeletal muscle. A peptide of similar size has been predicted from a splice variant of VAPB, termed VAPC. However, the peptide used to generate the VAPB anti-serum is not present in VAPC (16), and the VAPA anti-sera does not cross react significantly with *vapB*-derived species (see Supplementary Fig 1). It is concluded that these smaller molecular weight immunoreactive species are most likely generated by proteolysis of the VAP proteins. It has been shown previously that both VAPA and VAPB are enriched on the ER membrane (13, 15, 21). A distinct sub-cellular distribution for the two proteins is seen by co-immunostaining of HEK293 cells (Fig. 1B). Both proteins are localised in a

reticular pattern, but they exhibit only a modest level of co-localization. This distinct sub-cellular distribution of VAPA and VAPB is most striking in skeletal muscle (Fig1C). Fluorescent immunocytochemistry indicates a complementary distribution of VAPA and VAPB in the sarcoplasmic reticulum. VAPA is enriched on the A-and H-bands and the Z-line, while VAPB is restricted to the I-band and T-system regions (Fig1D). The I-band is enriched for IP₃ receptors and RyR localise mainly at the T-system (39), VAPA and VAPB may therefore, be associated with distinct intracellular calcium stores.

Interactions of the VAP MSP domain.

The ALS8- associated mutation in the VAPB protein lies within a highly conserved region of the MSP domain. In a previous series of experiments we had observed that, when expressed as an EGFP fusion protein, the MSP domains of both VAPA and VAPB formed intensely fluorescent, large intracellular aggregates, and were toxic to HEK293 and PC12 cell lines, and to primary cultures of rodent hippocampal neurons (Skehel, unpublished). To investigate possible mechanisms of the MSP domain toxicity a yeast two-hybrid screen was done to identify potential MSP interacting proteins. A sequence corresponding to amino acids 1-107 of mouse VAPA was used to screen a rat brain cDNA library. In addition to a number of FFAT- and MSP domain-containing proteins, a partial clone of the ER stress regulated transcription factor ATF6 was identified (26).

To characterize this interaction further, expression constructs for full length VAPA, VAPB and ATF6 were analysed by a fluorescent peptide complementation assay (27)(Fig 2). In this assay, a fluorescent protein is generated from the two separate parts of a split GFP, termed Venus1 and Venus2, only by the association of

two test polypeptides expressed as fusion proteins. A functional fluorescent protein is only generated when the two test proteins directly interact. Although the initial yeast two-hybrid interaction was between a truncated form of ATF6 and the MSP domain of VAPA, an interaction between full-length forms of VAPA and VAPB with ATF6 was readily detectable (Fig 2). Similarly, the ALS8-associated mutant VAPB^{P56S} was shown to be capable of interacting with ATF6 (Fig 2). No interaction was detected between VAPA, VAPB or ATF6 when co-expressed with heterologous leucine zipper-Venus fusions. The reconstitution of a fluorescent protein clearly indicates that VAPA and VAPB are capable of interacting with ATF6. Similar results were also obtained with the converse Venus combinations, where ATF6 was expressed as a fusion with Venus 1, and the VAP proteins were fused to Venus 2 (data not shown)(27).

Fluorescence analysis of HEK293 cells expressing EGFP-VAPB and FLAG-tagged ATF6 shows extensive regions of co-localization on the ER, but also some complementary distribution (Fig 3). The aggregates of EGFP-VAPB^{P56S} show some but not extensive co-localization with ATF6, although we cannot discount that low antigen accessibility may contribute to reduced ATF6 detection in VAPB^{P56S} aggregates. Expression of VAPB^{P56S} does not appear to cause gross disruption of ATF6 distribution in the ER (Fig 3).

ATF6 is inhibited by VAPB and VAPB^{P56S}.

ATF6 is one of a family of transmembrane transcription factors (28). It functions in a regulated transcription pathway involved in ER homeostasis and response to stress known as the Unfolded Protein Response (UPR)(29-31). Upon

accumulation of unfolded proteins in the lumen of the ER, ATF6 translocates from the ER to the Golgi and is proteolyzed in turn by S1P and S2P. This results in the release of the DNA binding and transcription transactivation domain of ATF6 from the ER membrane allowing it to enter the nucleus and activate transcription (26, 32).

ATF6 appears to interact with several promoter elements (30, 33, 34). A synthetic promoter has been generated that acts as an ATF6/XBP1 dependent transcription reporter (30). To determine if the interaction with VAPB affects the ability of ATF6 to activate transcription, luciferase-based transient transcription assays were done using this ATF6/XBP1-dependent reporter of transcription (30). In HEK293 cells basal levels of transcription from this promoter are reduced by over-expression of myc-tagged forms of VAPB or VAPB^{P56S} (Fig 4a). ATF6/XBP1-mediated transcription activated by the glycosylation inhibitor, tunicamycin, was also significantly reduced by over expression of VAPB or VAP-B^{P56S} (Fig 4a) (35, 36). Increasing levels of ATF6 by co-expression of a FLAG-tagged recombinant form of human ATF6 (37) increased basal and tunicamycin-induced expression from the ATF6/XBP1 reporter. In both cases the elevated levels of ATF6/XBP1 dependent transcription were also reduced by over expression of either VAPB or VAPB^{P56S} (Fig. 4b). This effect requires the cytoplasmic domains of VAPB and does not appear to be a non-specific consequence of increasing levels of protein in the ER membrane since over expression of a DsRed fluorescent fusion protein of the C-terminal hydrophobic domain of VAPB does not reduce the basal or tunicamycin-induced expression from the ATF6/XBP1 reporter (Fig 4a and Supp. data S3). Over expression of VAP proteins does not reduce expression levels of luciferase directed from a CMV promoter, therefore the repressive affect on the ATF6/XBP1 reporter is unlikely to be a the result of a general repression of transcription (Supp. data S4).

A similar inhibitory affect was also seen in the motor neuron derived cell line NSC34 (Fig4 c,d). In NSC34 cells basal levels of expression from the ATF6/XBP1 reporter are less than in HEK293, perhaps indicating lower levels of endogenous ATF6.

Consistent with the inhibitory affect seen by over expression of VAPB, siRNA-mediated reduction of endogenous VAPB results in an increase of basal and induced levels of ATF6/XBP1-dependent transcription (Fig 5).

When equal amounts of expression plasmid DNA for VAPB and VAPB^{P56S} were used for cell-transfections, the overall level of attenuation was similar between the wild type and mutant forms of VAPB (Fig 4). Immunoblot analysis of total protein from transfected cells, however, indicated that the mutant protein, VAPB^{P56S} - myc, accumulated to significantly lower levels, reaching only 20% of the level of wild type protein. (Fig 6). This suggests that VAPB^{P56S}-myc may exert a stronger inhibition on ATF6 than the wild type VAPB-myc, since a similar level of inhibition is achieved from a lower amount of protein. The difference in protein levels is less pronounced when VAPB and VAPB^{P56S} are expressed as EGFP fusion proteins (Fig 6), which indicates that the presence of the GFP moiety may have a stabilizing affect on VAP-B^{P56S}. Consistent with this, the inhibition of ATF6/XBP1-dependent transcription is more pronounced for EGFP-VAPB^{P56S} than EGFP-VAPB (Fig 6). Thus VAPB^{P56S} appears to have a significantly greater inhibitory affect on ATF6 mediated transcription than wild type VAPB. These results suggest that mis-regulation of ER stress responses may be important for the pathological affect of VAPB^{P56S} that leads to motor neuron degeneration.

Discussion.

The identification of a mutated gene responsible for a familial form of motor neuron disease greatly facilitates molecular and cellular studies of potential disease mechanisms. Understanding the cellular function of VAPB may indicate what molecular and cellular events are associated with the disease process of ALS8. It is likely that this information will be of relevance to both the inherited condition and the more common sporadic forms of disease.

Previous studies have demonstrated a role for VAP proteins on the ER. The N-terminal MSP domain contains an FFAT-motif binding site (21). This interaction has been shown to localize a number of cytoplasmic lipid-binding proteins to the ER and ER-derived membranes (18-20, 38). FFAT-dependent interactions between VAPA and Nir2 and 3 have also been shown to affect the gross structure of the ER (22). Both VAPA and VAPB appear to be expressed at different relative levels in specific tissues ((25) (16) and this study). Both proteins are enriched on the ER and co-localise to a large extent (24). There are, however, many regions where the two proteins do not co-localize, suggesting they are present in distinct functional regions of the ER. This is most clearly seen in skeletal muscle where VAPA is enriched within the A and H bands and Z-line, whereas VAPB is seen predominantly in the I-bands and T-region. The localization of VAPA is similar to that of the IP₃ receptor (39), whereas VAPB more closely resembles the distribution of Ryanodine receptors (40). Any disruption of VAPB function caused by the P56S mutation associated with ALS8 might, therefore, affect intracellular Ca²⁺ storage and Ca²⁺ signalling capacities. Intracellular Ca²⁺ levels have been implicated in many degenerative conditions (reviewed in (41)), and inhibition of Ryanodine receptor activity has been recently suggested as a possible pathological mechanism for motor neuron disease (42).

The proline residue at codon 56 within the MSP domain does not appear to contribute directly to FFAT-binding but co-immunoprecipitation of FFAT-containing proteins is reduced for VAPB^{P56S} (24). Perturbation of FFAT-dependent association with the ER could disrupt the sorting of lipids within and between cellular membranes (19, 20). A phosphoinositide-binding activity has been identified in the MSP domain of the yeast protein SCS2, that is a homologue of VAPA and VAPB (43).

Disruption of the MSP domain in VAPB^{P56S} could affect a similar activity in the mammalian proteins. Changes in membrane composition have been suggested as a cause of neurodegeneration (44), and hyperlipidemia is one of the clinical effects reported for VAPB^{P56S} families (3). Disruption of ER and Golgi structure and/or function has been suggested previously as a possible pathological mechanism for degenerative diseases of neurons (45-47). More recently ER stress in particular has been associated with sporadic and experimental models of motor neuron disease (48-50), and neurodegeneration in general (for reviews see(46, 47, 51)). A recent report has also suggested that VAPB levels may induce the ER Unfolded Protein Response by affecting the activity of IRE1(23). In this report we show that VAPA and VAPB can interact directly with the ER-localized transcription factor ATF6. Moreover, increasing the expression of VAPB attenuates the activity of ATF6, while reducing VAPB levels enhance ATF6-dependent transcription. Over expression of the mutant protein VAPB^{P56S} appears to attenuate the activity of ATF6 more profoundly than does wild type VAPB. The proteinaceous aggregates formed by VAPB^{P56S} do not appear to sequester ATF6 to a significant extent. The enhanced inhibitory affect of VAPB^{P56S} levels on ATF6 activity may not, therefore, be due simply to a reduction in

available ATF6. There are a number of stages in the activation of ATF6 that VAPB could influence. In response to accumulation of unfolded protein in the ER lumen ATF6 translocates from the ER to the Golgi. There it is sequentially processed by S1P and S2P proteases to release a C-terminal portion of the protein containing DNA binding and transactivation domains (32). The luminal N-terminal domain of ATF6 is required to detect the accumulation of unfolded proteins in the lumen of the ER. As VAPB has very little luminal structure it is unlikely to directly inhibit the ability of ATF6 to detect ER stress. Over expression of VAPB can disrupt membrane trafficking and so may indirectly inhibit the activation of ATF6 by reducing the translocation of ATF6 to the Golgi (15). Alternatively, VAP proteins might directly inhibit the translocation of ATF6 to the Golgi. It is also possible that VAP acts after translocation of ATF6 to the Golgi by a mechanism similar to that of Nucleobindin1 which represses S1P activation of ATF6 (53).

VAPB may act at the level of transcription. The yeast VAP homologue SCS2, originally identified as a suppressor of inositol auxotrophy, has been shown to localise activated genes to the nuclear membrane via an interaction with a FFAT domain-containing protein, Opi1 (10, 54). The localization to the nuclear membrane was essential for gene expression (54). If an analogous situation existed in mammals, over expression of VAPB could directly affect the activity of ATF6 at promoters adjacent to the nuclear membrane.

A regulatory role for VAP proteins on the surface of the ER.

The UPR and ERAD systems respond to the environment of the lumen of the ER. Perhaps the interaction between the VAP proteins and ATF6 represents an additional element of ER regulation that responds to levels of proteins associating with the

surface of the ER, or to proteins that do not have significant amounts of luminal structure.

VAP proteins interact with a broad range of other coiled-coil containing proteins such as VAMP/Synaptobrevin and syntaxin (12). If interactions of the coiled/coil domain also affected the MSP domain-dependent inhibition of ATF6, they could enable the levels of membrane proteins on the surface of the ER to activate ATF6.

VAP proteins and Hepatitis C virus replication.

The Hepatitis C virus has exploited potential structural and regulatory functions of the VAP proteins. Hepatitis C replicates in association with the ER. Two of the viral proteins required for this association, NS5A and NS5B, can bind to both VAPA and B, interacting with the coiled-coil and MSP domains respectively (56, 57). Disrupting these interactions or down regulating VAPA and VAPB protein levels inhibits virus replication (57, 58). Hepatitis C protein expression can also induce ER stress, activating both ATF6 and XBP1. This does not lead to a full Unfolded Protein Response (59, 60), and it has been suggested that mis-regulation of the ER stress response may in someway favour viral replication (60). Perhaps a similar mechanism may contribute to the pathogenesis of VAPB^{P56S}. The mutant protein could lead to a mis-regulation of ER stress regulatory pathways via aberrant ATF6 activity. Such mis-regulation could also have a role in the pathological affects of Hepatitis C infection.

ATF6 activity and neurodegeneration.

The increased level of ATF6 inhibition by VAP^{P56S} suggests that a possible pathological mechanism for ALS8 is mis-function of homeostatic regulatory systems of the ER. Kanekura *et al.*, recently demonstrated that increased VAPB levels could induce the unfolded protein response as indicated by activation of XBP1, and that the affect of VAPB^{P56S} was to diminish this activation (23). Our study suggests that VAP proteins can also affect the activity of ATF6, and that the mutation VAPB^{P56S} may, have a greater effect than the wild type protein VAPB. From gene transcription analysis on the UPR in *C.elegans* it has been shown that ATF6 mainly contributes to tonic levels of gene expression (61). In mammals ATF6 appears to have a more extensive role in the ER stress response, where it is required for the induced expression of principal ER chaperones, and also acts as a heterodimer with XBP1 to induce components of the ER associated degradation pathway (ERAD)(29).

The direct interaction between VAP proteins and ATF6 represents a previously uncharacterised mechanism for the regulation of transcriptional responses made to changes in ER metabolism. Over all, VAP proteins may have structural and regulatory functions based on interactions of the MSP domain. The pathological mechanism in ALS8, therefore, may be the result of an inability to deal appropriately with different forms of ER stress.

Materials and Methods.

Antisera. VAPB specific anti-serum was raised in sheep to a Multi Antigenic Peptide (MAP) form of a peptide corresponding to amino acids 174-189 of mouse VAPB (Alta Bioscience). This sequence is identical in rats and mice. The serum was affinity purified using the immunizing peptide. The VAPA anti-serum has been described previously (13). Anti-myc was monoclonal 9E10 and anti-FLAG was M2 (Sigma).

Muscle staining

Muscle tissue was fixed in 0.1M PBS containing 4% paraformaldehyde for 1-2 hours. Muscles were blocked in 4% BSA and 0.5% Triton-X (both Sigma) in PBS for 30 min before incubation in primary antibodies overnight at 4°C. The primary antibodies used were sheep anti-VAPB (1:200) and rabbit anti-VAPA, (1:300). After washing for 30 min in blocking solution, muscles were incubated for 4-5 hours in PBS containing secondary antibodies. The secondary antibodies used were Donkey anti-Sheep Cy2 (1:100, Jackson Laboratories) and Donkey anti-Rabbit Cy3 (1:100, Jackson Laboratories). After a 2 hr wash in PBS, muscles were mounted on glass slides in mowoil mounting medium (2.4g mowoil (Poly vinyl Alcohol, Calbiochem), 6g glycerol, 2.5% 1,4-diazobicyclo-octane (DABCO, antifade, Sigma), 12 ml 200mM Tris (pH 8,5)). Preabsorption experiments for VAPB were performed using a 100-fold excess of the VAPB peptide (~40mg/ml). This was added to the antibody and left at room temperature for 1 hour before proceeding with the remainder of the immunocytochemistry protocol detailed above.

Preparations were analysed using a laser confocal scanning microscope (Biorad Radiance 2000). The strobing function was always enabled to prevent signal bleeding through from one channel to another. Confocal z-series were merged using Laserssharp (Biorad) software. All images were analysed and prepared for presentation in Adobe Photoshop.

Cell Staining

HEK293 cells grown on poly-D-lysine coated cover slips were fixed in 3% paraformaldehyde, 0.03% glutaraldehyde (w/v) in PBS, at room temperature for 20mins. Fixative was quenched and cells permeabilized with a solution of 50mM NH_4Cl , 0.2% (w/v) Saponin (Sigma), for 15 minutes at room temperature. Cells were washed, and antibodies diluted in a solution containing 0.2% (w/v) fish skin gelatin (Sigma G-7765), 0.02% saponin, in PBS. Inverted cover slips were mounted in Mowiol, and examined on a Zeiss Imager.Z1 microscope fitted with a LSM 510 Meta confocal excitation/acquisition system.

Peptide complementation

Full length coding sequences for mouse VAPA, VAPB, VAPA^{P56S}, VAPB^{P56S}, and human ATF6a (NM_007348) were amplified in a PCR that introduced flanking BspEI and XbaI, or NotI and ClaI restriction sites, and sub-cloned into pcDNA3.1(zeo)-Venus[1] or pcDNA3.1(zeo)-Venus[2] respectively (27). HEK293 were transfected using Lipofectamine 2000 (Invitrogen). For each transfection 200ng of total DNA was used. Images of living cells were acquired 24 hours after transfection on an

Olympus IX70 fluorescence microscope using Openlab software (Improvision).

Representative images are shown.

Transcription assay

HEK293 or NSC-34 cells were grown in Dulbecco's Modified Eagle's Medium supplemented with 10% fetal bovine serum. Cells were transfected using Lipofectamine2000 (Invitrogen). Each transfection mixture contained 300 ng of p5xATF6-GL3 (30) and 100ng of the internal control renilla luciferase reporter, pRL-TK. VAPB and VAPB^{P56S} were expressed as EGFP-fusion proteins derived from pEGFP-C1 (Clontech), or as myc epitope tagged fusion proteins where the EGFP coding sequence was replaced with a myc epitope coding sequence. The total amount of DNA per transfection was 500ng . ATF6 was over expressed as a FLAG-tagged fusion protein from pCMV-ATF6-3xFLAG7.1 (62). 100ng of each VAPB and ATF6 expression plasmid was used, with the total amount of DNA in each transfection made up to 600ng with the vector pEGFP-C3 (Clontech). 24 hours after transfection ER stress was induced for 12 hours with 2mg/ml tunicamycin (Calbiochem). Cells were then lysed and assayed for firefly and renilla luciferase activity using the Dual GloTM Luciferase Assay System (Promega). Firefly and renilla luminescence were measured using a FLUOstar OPTIMA micro-plate reader (BMG LABTECH). Firefly luciferase luminescence values are normalised to renilla firefly luminescence values and are averages of 4 experiments with S.E.

siRNA transfection

10⁶ HEK293 cells were nucleofected with 200 pMoles of VAPB siRNA (Quiagen) or a control GFP-siRNA (Dharmacon) using the Amaxa Biosystems nucleofector. 24 hours after nucleofection, cells were transfected with p5xATF6-GL3 and pRLTK as described above. After a further 24 hours, cells were treated with 2 µg/ml Tunicamycin (Calbiochem) for 12 hours and then assayed for luciferase activity as above.

Acknowledgments.

The authors wish to thank and acknowledge Dr. Francesc Soriano, Dr. Giles Hardingham and Dr. Mandy Jackson for help and advice during the course of this work. Prof. Ron Prywes generously supplied pCMV-ATF6-3xFLAG7.1 and p5xATF6-GL3. Prof. Steve Michnick generously supplied the plasmid vectors of the Peptide Complementation assays. The work was supported by The Wellcome Trust (Grant number 063502), Scottish Motor Neuron Disease Association, BBSRC (THG) Medical Research Scotland (THG), and The Medical Research Council (SM).

Conflict of interest.

The authors declare no conflicts of interest regarding any aspect of the presented work.

References

1. Nishimura, A.L., Mitne-Neto, M., Silva, H.C., Richieri-Costa, A., Middleton, S., Cascio, D., Kok, F., Oliveira, J.R., Gillingwater, T., Webb, J. *et al.* (2004) A mutation in the vesicle-trafficking protein VAPB causes late-onset spinal muscular atrophy and amyotrophic lateral sclerosis. *Am. J. Hum. Genet.*, 75, 822-831.
2. Nishimura, A., Mitne-Neto, M., Silva, H., Oliveira, J., Vainzof, M. and Zatz, M. (2004) - A novel locus for late onset amyotrophic lateral sclerosis/motor neurone. *J. Med. Genet.*, 41, 315-320.
3. Marques, V.D., Barreira, A.A., Davis, M.B., Abou-Sleiman, P.M., Silva, W.A., Jr., Zago, M.A., Sobreira, C., Fazan, V. and Marques, W., Jr. (2006) Expanding the phenotypes of the Pro56Ser VAPB mutation: proximal SMA with dysautonomia. *Muscle Nerve*, 34, 731-739.
4. Logroscino, G., Beghi, E., Zoccolella, S., Palagano, R., Fraddosio, A., Simone, I.L., Lamberti, P., Lepore, V., Serlenga, L. and the, S.r. (2005) Incidence of amyotrophic lateral sclerosis in southern Italy: a population based study. *J. Neurol. Neurosurg. Psychiatry.*, 76, 1094-1098.
5. (2001) Incidence of ALS in Italy: Evidence for a uniform frequency in Western countries. *Neurology*, 56, 239-244.
6. Bradley, W.G. (1995) Overview of motor neuron disease: classification and nomenclature. *Clinical neuroscience (New York, N.Y.*, 3, 323-236.
7. Swash, M. and Desai, J. (2000) Motor neuron disease: classification and nomenclature. *Amyotroph. Lateral Scler. Other Motor Neuron Disord.*, 1, 105-112.

8. Schymick, J.C., Talbot, K. and Traynor, B.J. (2007) Genetics of sporadic amyotrophic lateral sclerosis. *Hum. Mol. Genet.*, 16, R233-242.
9. Skehel, P., Martin, K., Kandel, E. and Bartsch, D. (1995) - A VAMP-binding protein from *Aplysia* required for neurotransmitter release. *Science*, 269, 1580-1583.
10. Kagiwada, S., Hosaka, K., Murata, M., Nikawa, J. and Takatsuki, A. (1998) The *Saccharomyces cerevisiae* SCS2 gene product, a homolog of a synaptobrevin-associated protein, is an integral membrane protein of the endoplasmic reticulum and is required for inositol metabolism. *J. Bacteriol.*, 180, 1700-1708.
11. Pennetta, G., Hiesinger, P., Fabian-Fine, R., Meinertzhagen, I. and Bellen, H. (2002) - *Drosophila* VAP-33A directs bouton formation at neuromuscular junctions in. *Neuron*, 35, 291-306.
12. Weir, M., Xie, H., Klip, A. and Trimble, W. (2001) - VAP-A binds promiscuously to both v- and tSNAREs. *Biochem. Biophys. Res. Commun.*, 286, 616-621.
13. Skehel, P., Fabian-Fine, R. and Kandel, E. (2000) - Mouse VAP33 is associated with the endoplasmic reticulum and microtubules. *Proc. Natl. Acad. Sci. U S A*, 97, 1101-1106.
14. Laurent, F., Labesse, G. and Wit, P.d. (2000) - Molecular cloning and partial characterization of a plant VAP33 homologue. *Biochem. Biophys. Res. Commun.*, 270, 286-292.
15. Soussan, L., Burakov, D., Daniels, M., Toister-Achituv, M., Porat, A., Yarden, Y. and Elazar, Z. (1999) - ERG30, a VAP-33-related protein, functions in protein transport mediated. *J. Cell. Biol.*, 146, 301-311.

16. Nishimura, Y., Hayashi, M., Inada, H. and Tanaka, T. (1999) Molecular Cloning and Characterization of Mammalian Homologues of Vesicle-Associated Membrane Protein-Associated (VAMP-Associated) Proteins. *Biochem. Biophys. Res. Commun.*, 254, 21-26.
17. Sepsenwol, S., Ris, H. and Roberts, T.M. (1989) A unique cytoskeleton associated with crawling in the amoeboid sperm of the nematode, *Ascaris suum*. *J. Cell. Biol.*, 108, 55-66.
18. Loewen, C., Roy, A. and Levine, T. (2003) - A conserved ER targeting motif in three families of lipid binding proteins. *Embo J.*, 22, 2025-2035.
19. Wyles, J., McMaster, C. and Ridgway, N. (2002) - Vesicle-associated membrane protein-associated protein-A (VAP-A) interacts. *J. Biol. Chem.*, 277, 29908-29918.
20. Kawano, M., Kumagai, K., Nishijima, M. and Hanada, K. (2006) Efficient trafficking of ceramide from the endoplasmic reticulum to the Golgi apparatus requires a VAMP-associated protein-interacting FFAT motif of CERT. *J. Biol. Chem.*, 281, 30279-30288.
21. Kaiser, S.E., Brickner, J.H., Reilein, A.R., Fenn, T.D., Walter, P. and Brunger, A.T. (2005) Structural basis of FFAT motif-mediated ER targeting. *Structure*, 13, 1035-1045.
22. Amarilio, R., Ramachandran, S., Sabanay, H. and Lev, S. (2005) Differential regulation of endoplasmic reticulum structure through VAP-Nir protein interaction. *J. Biol. Chem.*, 280, 5934-5944.
23. Kanekura, K., Nishimoto, I., Aiso, S. and Matsuoka, M. (2006) Characterization of amyotrophic lateral sclerosis-linked P56S mutation of

- vesicle-associated membrane protein-associated protein B (VAPB/ALS8). *J. Biol. Chem.*, 281, 30223-30233.
24. Teuling, E., Ahmed, S., Haasdijk, E., Demmers, J., Steinmetz, M.O., Akhmanova, A., Jaarsma, D. and Hoogenraad, C.C. (2007) Motor neuron disease-associated mutant vesicle-associated membrane protein-associated protein (VAP) B recruits wild-type VAPs into endoplasmic reticulum-derived tubular aggregates. *J. Neurosci.*, 27, 9801-9815.
 25. Weir, M., Klip, A. and Trimble, W. (1998) - Identification of a human homologue of the vesicle-associated membrane. *Biochem. J.*, 333, 247-251.
 26. Yoshida, H., Haze, K., Yanagi, H., Yura, T. and Mori, K. (1998) Identification of the cis-acting endoplasmic reticulum stress response element responsible for transcriptional induction of mammalian glucose-regulated proteins. Involvement of basic leucine zipper transcription factors. *J. Biol. Chem.*, 273, 33741-33749.
 27. Remy, I., Galarneau, A. and Michnick, S.W. (2002) Detection and visualization of protein interactions with protein fragment complementation assays. *Methods. Mol. Biol.*, 185, 447-459.
 28. Bailey, D. and O'Hare, P. (2007) Transmembrane bZIP Transcription Factors in ER Stress Signaling and the Unfolded Protein Response. *Antioxid. Redox. Signal.*
 29. Yamamoto, K., Sato, T., Matsui, T., Sato, M., Okada, T., Yoshida, H., Harada, A. and Mori, K. (2007) Transcriptional induction of mammalian ER quality control proteins is mediated by single or combined action of ATF6alpha and XBP1. *Developmental Cell*, 13, 365-376.

30. Wang, Y., Shen, J., Arenzana, N., Tirasophon, W., Kaufman, R.J. and Prywes, R. (2000) Activation of ATF6 and an ATF6 DNA binding site by the endoplasmic reticulum stress response. *J. Biol. Chem.*, 275, 27013-27020.
31. Ron, D. and Walter, P. (2007) Signal integration in the endoplasmic reticulum unfolded protein response. *Nature Rev. Cell. Biol.*, 8, 519-529.
32. Ye, J., Rawson, R.B., Komuro, R., Chen, X., Dave, U.P., Prywes, R., Brown, M.S. and Goldstein, J.L. (2000) ER stress induces cleavage of membrane-bound ATF6 by the same proteases that process SREBPs. *Molecular Cell*, 6, 1355-1364.
33. Hai, T.W., Liu, F., Coukos, W.J. and Green, M.R. (1989) Transcription factor ATF cDNA clones: an extensive family of leucine zipper proteins able to selectively form DNA-binding heterodimers. *Genes. Dev.*, 3, 2083-2090.
34. Yoshida, H., Okada, T., Haze, K., Yanagi, H., Yura, T., Negishi, M. and Mori, K. (2000) ATF6 activated by proteolysis binds in the presence of NF-Y (CBF) directly to the cis-acting element responsible for the mammalian unfolded protein response. *Mol. Cell. Biol.*, 20, 6755-6767.
35. Tkacz, J. (1981) *Antibiotics, Modes and Mechanisms of Microbial Growth Inhibitors*.
36. Haze, K., Yoshida, H., Yanagi, H., Yura, T. and Mori, K. (1999) Mammalian Transcription Factor ATF6 Is Synthesized as a Transmembrane Protein and Activated by Proteolysis in Response to Endoplasmic Reticulum Stress. *Mol. Biol. Cell*, 10, 3787-3799.
37. Shen, J., Snapp, E.L., Lippincott-Schwartz, J. and Prywes, R. (2005) Stable binding of ATF6 to BiP in the endoplasmic reticulum stress response. *Mol. Cell. Biol.*, 25, 921-932.

38. Loewen, C.J. and Levine, T.P. (2005) A highly conserved binding site in vesicle-associated membrane protein-associated protein (VAP) for the FFAT motif of lipid-binding proteins. *J. Biol. Chem.*, 280, 14097-14104.
39. Tasker, P.N., Michelangeli, F. and Nixon, G.F. (1999) Expression and Distribution of the Type 1 and Type 3 Inositol 1,4,5-Trisphosphate Receptor in Developing Vascular Smooth Muscle. *Circ. Res.*, 84, 536-542.
40. Lesh, R.E., Nixon, G.F., Fleischer, S., Airey, J.A., Somlyo, A.P. and Somlyo, A.V. (1998) Localization of Ryanodine Receptors in Smooth Muscle. *Circ. Res.*, 82, 175-185.
41. Mattson, M.P. (2007) Calcium and neurodegeneration. *Aging Cell*, 6, 337-350.
42. Kihira, T., Utunomiya, H. and Kondo, T. (2005) Expression of FKBP12 and ryanodine receptors (RyRs) in the spinal cord of MND patients. *Amyotrophic Lateral Sclerosis*, 6, 94 - 99.
43. Kagiwada, S. and Hashimoto, M. (2007) The yeast VAP homolog Scs2p has a phosphoinositide-binding ability that is correlated with its activity. *Biochem. Biophys. Res. Commun.* epublished ahead of print.
44. Koudinov, A.R. and Koudinova, N.V. (2005) Cholesterol homeostasis failure as a unifying cause of synaptic degeneration. *J. Neurol. Sci.*, 229-230, 233-40.
45. Mourelatos, Z., Gonatas, N.K., Stieber, A., Gurney, M.E., Dal Canto, M.C., Chen, Y., Gonatas, J.O., Appel, S.H., Hays, A.P., Hickey, W.F. *et al.* (1996) The Golgi apparatus of spinal cord motor neurons in transgenic mice expressing mutant Cu,Zn superoxide dismutase becomes fragmented in early, preclinical stages of the disease

Fragmentation of the Golgi apparatus of motor neurons in amyotrophic lateral sclerosis. *Proc. Natl. Acad. Sci. U S A*, 93, 5472-5477.

46. Paschen, W. and Frandsen, A. (2001) Endoplasmic reticulum dysfunction--a common denominator for cell injury in acute and degenerative diseases of the brain? *J. Neurochem.*, 79, 719-725.
47. Lehotsky, J., Kaplan, P., Babusikova, E., Strapkova, A. and Murin, R. (2003) Molecular pathways of endoplasmic reticulum dysfunctions: possible cause of cell death in the nervous system. *Physiol. Res.*, 52, 269-274.
48. Nagata, T., Ilieva, H., Murakami, T., Shiote, M., Narai, H., Ohta, Y., Hayashi, T., Shoji, M. and Abe, K. (2007) Increased ER stress during motoneuron degeneration in a transgenic mouse model of ALS. *Neurol. Res.*
49. Kikuchi, H., Almer, G., Yamashita, S., Guegan, C., Nagai, M., Xu, Z., Sosunov, A.A., McKhann, G.M., 2nd and Przedborski, S. (2006) Spinal cord endoplasmic reticulum stress associated with a microsomal accumulation of mutant superoxide dismutase-1 in an ALS model. *Proc. Natl. Acad. Sci. U S A*, 103, 6025-6030.
50. Ilieva, E.V., Ayala, V., Jove, M., Dalfo, E., Cacabelos, D., Povedano, M., Bellmunt, M.J., Ferrer, I., Pamplona, R. and Portero-Otin, M. (2007) Oxidative and endoplasmic reticulum stress interplay in sporadic amyotrophic lateral sclerosis. *Brain*. epublished ahead of print.
51. Yoshida, H. (2007) ER stress and diseases. *FEBS Journal*, 274, 630-658.
52. Bailey, D., Barreca, C. and O'Hare, P. (2007) Trafficking of the bZIP Transmembrane Transcription Factor CREB-H into Alternate Pathways of ERAD and Stress-Regulated Intramembrane Proteolysis. *Traffic*, 8, 1796-814.
53. Tsukumo, Y., Tomida, A., Kitahara, O., Nakamura, Y., Asada, S., Mori, K. and Tsuruo, T. (2007) Nucleobindin 1 Controls the Unfolded Protein Response by Inhibiting ATF6 Activation. *J. Biol. Chem.*, 282, 29264-29272.

54. Brickner, J.H. and Walter, P. (2004) Gene recruitment of the activated INO1 locus to the nuclear membrane. *PLoS Biol*, 2, e342.
55. Brunger, A.T. (2005) Structure and function of SNARE and SNARE-interacting proteins. *Quarterly reviews of biophysics*, 38, 1-47.
56. Gao, L., Aizaki, H., He, J. and MMLai (2004) - Interactions between viral nonstructural proteins and host protein hVAP-33. *J. Virol*, 78, 3480-3488.
57. Hamamoto, I., Nishimura, Y., Okamoto, T., Aizaki, H., Liu, M., Mori, Y., Abe, T., Suzuki, T., Lai, M.M., Miyamura, T. *et al.* (2005) Human VAP-B is involved in hepatitis C virus replication through interaction with NS5A and NS5B. *J. Virol*, 79, 13473-13482.
58. Zhang, J., amada, O., Sakamoto, T., Yoshida, H., Iwai, T., Matsushita, Y., Shimamura, H., Araki, H. and Shimotohno, K. (2004) - Down-regulation of viral replication by adenoviral-mediated expression of. *Virology*, 320, 135-43.
59. Tardif, K.D., Mori, K. and Siddiqui, A. (2002) Hepatitis C virus subgenomic replicons induce endoplasmic reticulum stress activating an intracellular signaling pathway. *J. Virol*, 76, 7453-7459.
60. Zheng, Y., Gao, B., Ye, L., Kong, L., Jing, W., Yang, X., Wu, Z. and Ye, L. (2005) Hepatitis C virus non-structural protein NS4B can modulate an unfolded protein response. *Journal of microbiology (Seoul, Korea)*, 43, 529-36.
61. Shen, X., Ellis, R.E., Sakaki, K. and Kaufman, R.J. (2005) Genetic interactions due to constitutive and inducible gene regulation mediated by the unfolded protein response in *C. elegans*. *PLoS genetics*, 1, e37.

62. Shen, J., Chen, X., Hendershot, L. and Prywes, R. (2002) ER stress regulation of ATF6 localization by dissociation of BiP/GRP78 binding and unmasking of Golgi localization signals. *Developmental Cell*, 3, 99-111.

Figure legends.

Figure 1A. Detection of VAPA and VAPB in different tissues. Anti-peptide anti-serum was raised to residues 174-189 of mouse VAPB. In the tissues indicated the predominant immunoreactivity is at approximately 27kD, in agreement with the molecular weight predicted from the cDNA. Both VAPA and VAPB are expressed widely but at different levels. A faster migrating VAPB-related doublet signal of approximately 14kD is clearly detected in forebrain and cerebellum protein extracts. The immunoblot is deliberately over exposed to demonstrate the restricted nature of this expression pattern. A faster migrating immunoreactive species of approximately 14kD is also seen with VAPA anti-sera, however, in contrast to that seen for VAPB, this species is detectable in pancreas, liver, forebrain, lung and thymus, kidney and testis; low levels are seen in the cerebellum and no signal is detected in Heart or skeletal muscle.

Figure 1B. VAPA and VAPB are expressed in distinct reticular patterns. Indirect immunofluorescence analysis of VAPA and VAPB in HEK293 cells reveals a reticular pattern of expression, but detects very little co-localization of the two proteins. VAPA is shown in red and VAPB in green.

Figure 1C. VAPA and VAPB are enriched in a complementary distribution in skeletal muscle. Confocal micrographs of an immunocytochemically labelled transversus abdominis muscle from a 2 month old mouse (VAPA in red, VAPB in green). The staining patterns of VAPB were consistent with it being located around putative I—band and T-system regions. In contrast, VAPA was absent from these regions, and appeared to be more strongly expressed in the regions associated with A- and H-bands and Z-lines. A pseudo-coloured electron micrograph is shown to indicate the position of VAPA and VAPB staining in relation to the structure of a muscle sarcomere

Figure 2. Peptide complementation assay for the interaction of VAPA and VAPB with ATF6. The coding sequences of mouse VAPA, VAPB and VAPB^{P56S} were expressed in HEK293 cells as fusion proteins with a truncated non- fluorescent form of YFP, Venus 1 (Remy et al., 2002). These proteins were co-expressed with the complementary ATF6-Venus 2 fusion protein. Fluorescence indicates reconstitution of a functional YFP and therefore a direct interaction of VAPA and VAPB with ATF6. Wild type VAPB and mutant VAPB^{P56S} are capable of interacting with ATF6. Controls in which a homodimerizing leucine zipper peptide was expressed as either a Venus 1 or Venus 2 fusion proteins show no fluorescence when expressed with the complementary VAP or ATF6 fusion proteins. Bright field or fluorescence images were acquired from live cells through cell culture plastic.

Figure 3. Co-localization of VAPB and ATF6. HEK293 cells were transfected with FLAG-ATF6, EGFP-VAPB and EGFP-VAPB^{P56S}. In colour plates FLAG-ATF6 is shown in red and EGFP-VAPB or EGFP-VAPB^{P56S} is in green. There is extensive, but not total co-localisation of VAPB and ATF6 in a reticular distribution. ATF6 co-localises with the aggregates formed by VAPB^{P56S}, but not in a punctate pattern. Note that VAPB^{P56S} does not cause a gross change in the distribution of ATF6.

Figure 4. VAPB and VAPB^{P56S} inhibit transcription from an ATF6 regulated transcription reporter. (A) HEK293 were transfected with a reporter plasmid containing the luciferase cDNA regulated by five ATF6/XBP1 binding sites, pGL3(5X)ATF6. Cell cultures were co-transfected with expression plasmids encoding VAPB or VAPB^{P56S} as myc-tagged fusion proteins (VAPB-myc and VAPB^{P56S}-myc) or a monomeric red fluorescent fusion protein containing the C-terminal 41 amino acids of VAPB (VAPB-Cterm). Where indicated cultures were treated for 12 hours with 2mg/ml Tunicamycin to induce ER stress. VAPB and VAPB^{P56S} reduce constitutive levels of ATF6/XBP1 activity, while VAPB-Cterm had no effect. (B) Over expression of ATF6 as a ATF6-FLAG fusion protein increased basal and tunicamycin-induced activity of the ATF6/XBP1 reporter gene, but in both cases levels of activity were reduced by co-expression of VAPB-myc or VAPB^{P56S}-myc. (C and D) The same experiments using the motor neuron-like cell line NSC34 gave similar results.

Figure 5. VAPB siRNA reduces the levels of endogenous VAPB and increases basal ATF6/XBP1-dependent transcription. (A) Immunoblot analysis of HEK293 cells

nucleofected with VAPB siRNA or GFP siRNA and non-transfected cells shows a 25% reduction in levels of endogenous VAPB when treated with VAPB siRNA and no reduction in GFP siRNA treated cells. *A 60 KD non-specific band from longer exposures of the immunoblot serves as a loading control. Band intensities were measured using ImageJ (NIH). (B) siRNA to VAPB increases basal, and tunicamycin-induced, transcription and from an ATF6/XBP1-regulated transcription promoter.

Figure 6. VAPB^{P56S} accumulates to lower levels than VAPB. Immunoblot analysis of HEK293 cells expressing myc or GFP-tagged forms of VAPB and VAPB^{P56S}.

Duplicate samples are shown, and relative levels expressed as a histogram of signal intensities. As both myc and GFP fusion proteins VAPB^{P56S} accumulates to lower levels than VAPB. VAPB^{P56S}-myc is approximately 15% the level of VAPB-myc, and VAPB^{P56S}-GFP is approximately 50% the level of VAPB-GFP. The GFP moiety appears to have a stabilising affect on the levels of mutant protein, allowing it to accumulate to higher levels than the myc-tagged form. B. Consistent with this the inhibition of ATF6 reporter gene expression is reduced to a greater relative level by VAPB^{P56S}-GFP than VAPB^{P56S}-myc.

Band intensities were determined using ImageJ (NIH) Intensities for both myc and GFP, VAPB and VAPBP56S were normalised to the p38 loading control.

Figure 1A.

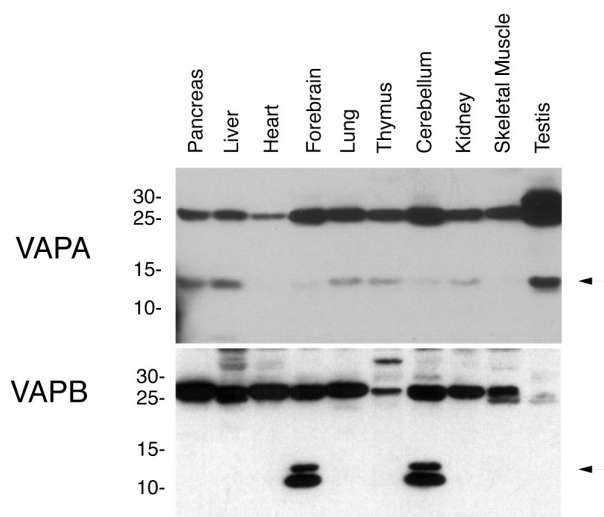


Figure 1B

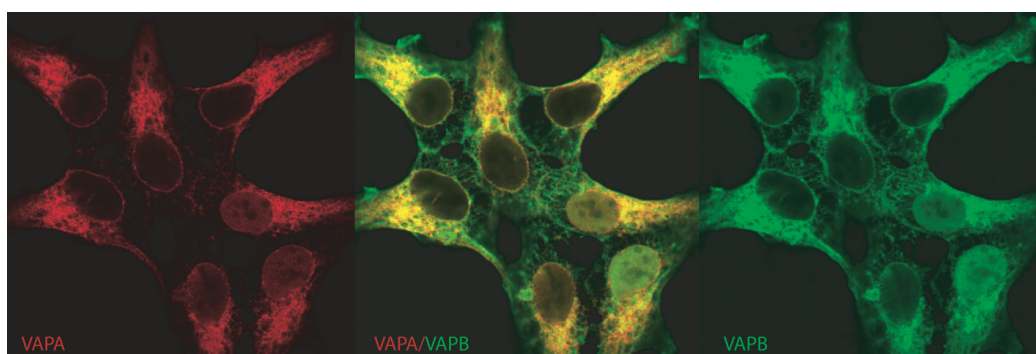


Figure 1 C

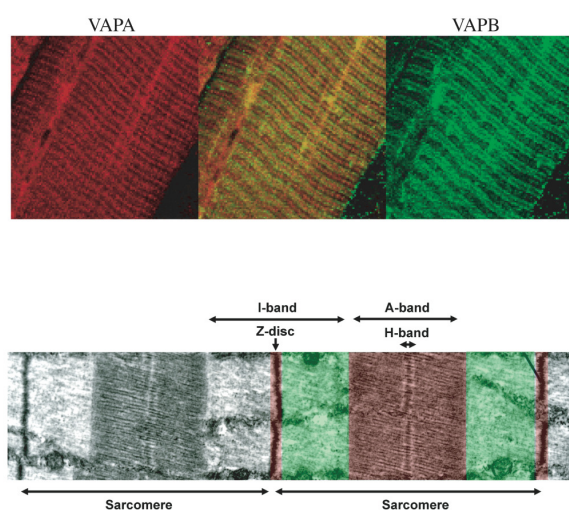


Figure 2.

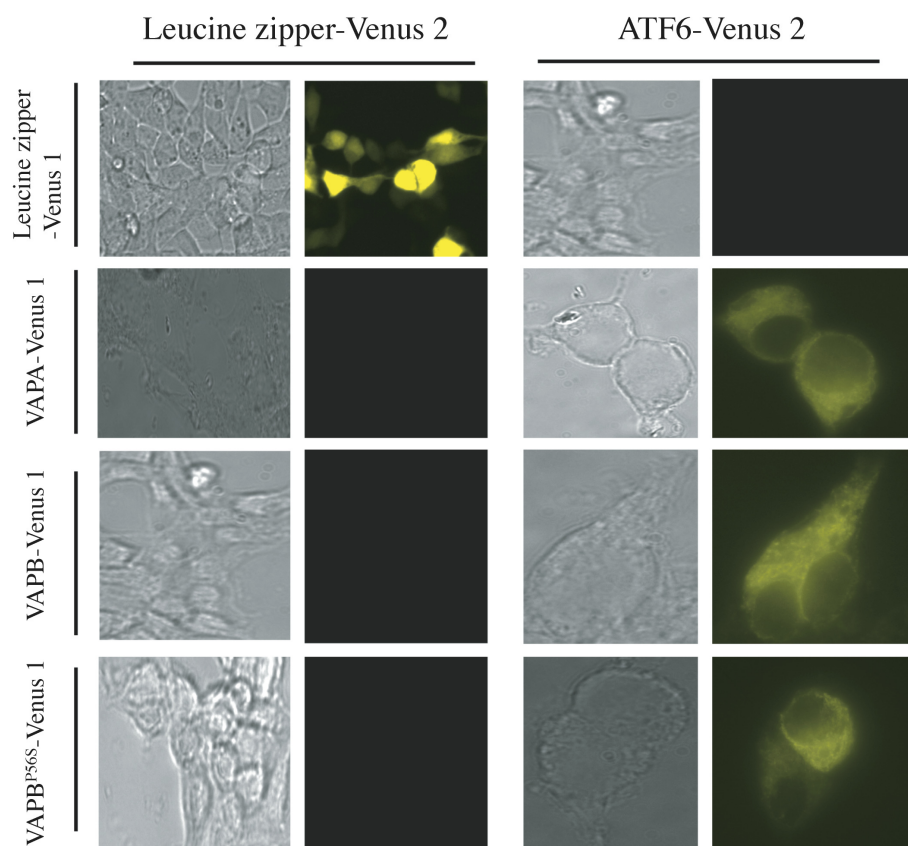


Figure 3

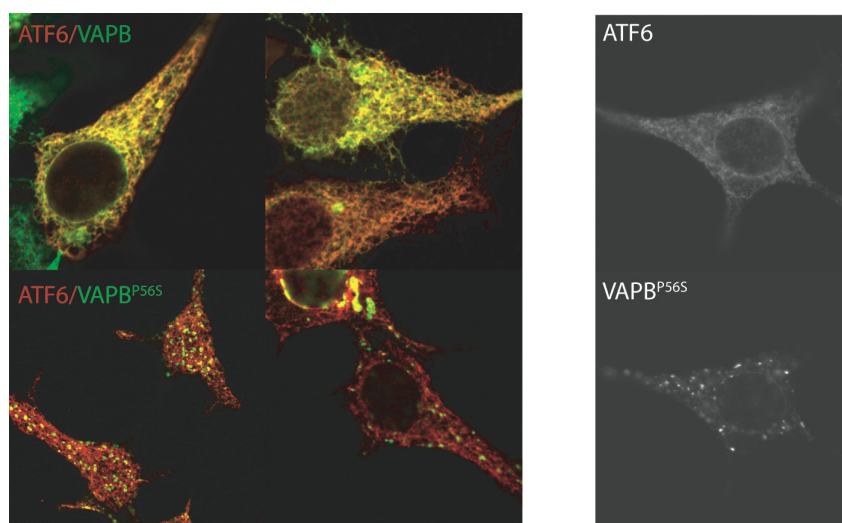


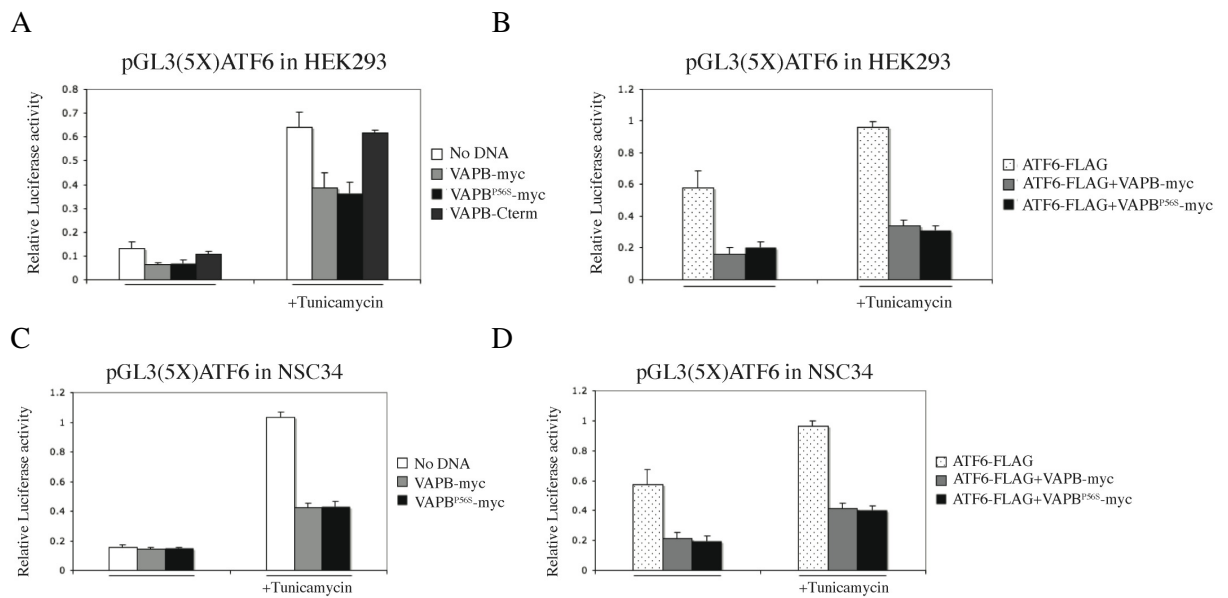
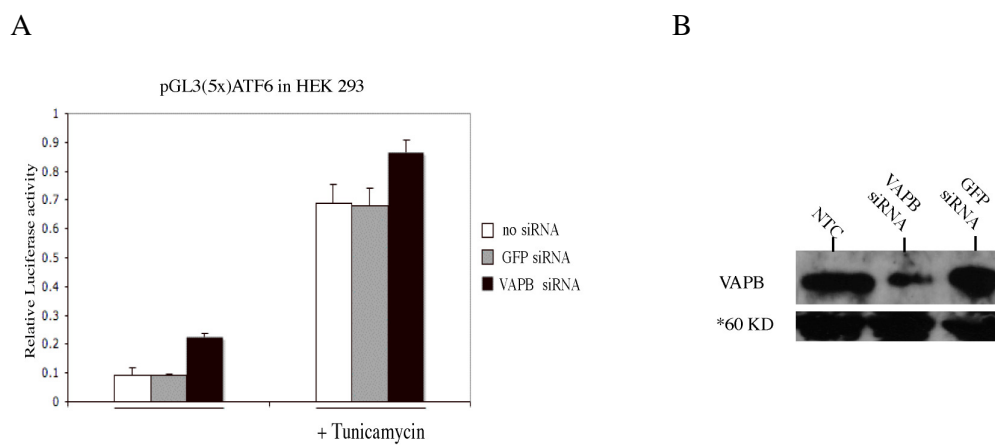
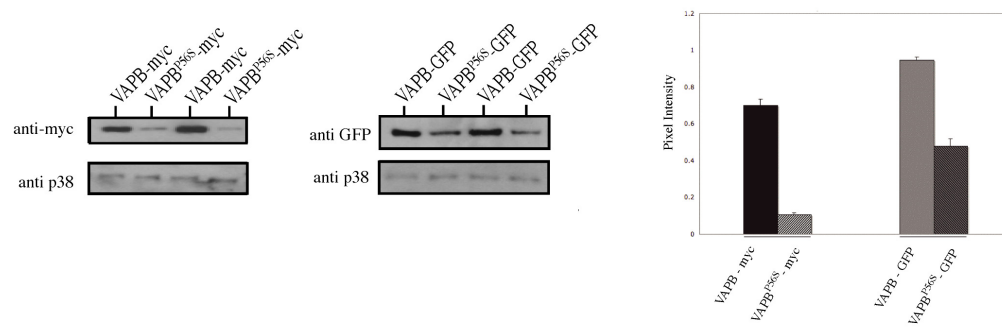
Figure 4**Figure 5**

Figure 6**A****B**